

## Salt-Enhanced Photocatalytic Hydrogen Production from Water with Carbon Nitride Nanorod Photocatalysts: Cation and pH Dependence

Xiaobo Li<sup>a,†</sup>, Stuart A. Bartlett<sup>a</sup>, James M. Hook<sup>b</sup>, Ivan Sergeev<sup>c</sup>, Edwin B. Clatworthy<sup>a</sup>, Anthony F. Masters<sup>a</sup>, Thomas Maschmeyer<sup>a</sup>

<sup>a</sup> Laboratory of Advanced Catalysis for Sustainability, School of Chemistry, The University of Sydney, Sydney, 2006, Australia

<sup>b</sup> Mark Wainwright Analytical Centre, and School of Chemistry, The University of New South Wales, Sydney, 2052, Australia

<sup>c</sup> Bruker Biospin Corporation, 15 Fortune Drive, Billerica, MA, USA, 01821

### Experimental details:

All chemicals used were reagent grade and were used as received.

The polymeric carbon nitride precursor was thermally polymerized in a tube furnace (Carbolite, GHA 12/300). UV-vis spectra were measured on a Varian Cary 5 UV/vis spectrophotometer. The instrument that measures the zeta potential is the Malvern Zetasizer Nano ZS. The instrument for photoluminescence is the Cary Eclipse Fluorescence Spectrometer. Surface area and porosity measurements were carried out on a Micromeritics Accelerated Surface Area and Porosimetry System 2020 instrument. Each sample was degassed at 120 °C, and nitrogen adsorption/desorption isotherms were collected at -196 °C. The BET surface areas were calculated from the adsorption branch of the isotherms by using the Micromeritics software. Powder XRD patterns were collected using a PANalytical X'Pert PRO MPD X-ray diffractometer using Cu K $\alpha$  ( $\lambda = 1.5419 \text{ \AA}$ ) radiation. Elemental Microanalysis was performed on Elemental Analyser, Model PE2400 CHNS/O (PerkinElmer, Shelton, CT, USA) with PC based data system, PE Datamanager 2400 for Windows<sup>TM</sup> and a PerkinElmer AD-6 Ultra Micro Balance. Dynamic light scattering characterization was collected on Malvern Instruments High Performance Particle Sizer.

## Synthesis of CNK

A two-step polymerization strategy was applied here. Initial precursor of CNK, melamine, which was loaded in an alumina crucible covered with a lid, was heated to 390 °C for 24 h with a ramp rate of 2.2 °C /min in a quartz tube with flowing N<sub>2</sub> gas at a flow rate of 100 ml/min. The obtained white solid is boiled in water with 10 vol% acetic acid overnight. After thoroughly washing with water, the white solid was dried and kept in a 110 °C oven for a second step polymerization. 1.5 g of the obtained white solid from the previous step was mixed and ground with 3.375 g LiCl and 4.125 g KCl, then, the mixture was loaded into a lid-covered crucible and heated to 400 °C in a flowing N<sub>2</sub> atmosphere at a flow rate of 100 ml/min with a ramping rate of 6.3 °C and kept at this temperature for an additional 6 h. Then, the temperature was further increased to 600 °C with a ramping rate of 6.7 K and kept for another 12 h. The mixture was cooled to room temperature under flowing N<sub>2</sub>. The solid obtained was washed in boiling water and collected following centrifugation at least three times. After drying the solid in at 110 °C in an oven overnight, a yellow solid was obtained.

## *Synthesis of conventional polymeric carbon nitrides*

### Synthesis of CN

The carbon nitride precursor, melamine, was loaded on an alumina boat with a lid and heated to 600 °C from room temperature with a ramp rate of 2.2 °C /min in a quartz tube (2.5 cm in diameter) with flowing N<sub>2</sub> gas at a flow rate of 100 ml/min and then held for 4 hr.

### Synthesis of CNP

PCN\_P was synthesized according to the literature.<sup>[1]</sup> Thus, cyanamide (12 g) was dissolved in a 40 % dispersion of 12 nm SiO<sub>2</sub> particles (Ludox HS40, Aldrich) in water (15 g) with stirring at 60 °C overnight. The resulting transparent mixture was then heated to and held at 550 °C over 4 h in N<sub>2</sub> with a ramp rate of 2.2 °C /min. The resulting brown-yellow powder was treated with aqueous 4 M NH<sub>4</sub>HF<sub>2</sub> solution for 36 hr to remove the silica template. The powder was then centrifuged, washed with distilled water and finally, dried at 80 °C in an oven.

## Synthesis of potassium melonate and cyamelurate

Potassium melonate was prepared according to a literature preparation.<sup>[2]</sup> Potassium cyamelurate was prepared according to a literature preparation.<sup>[3]</sup>

### Photocatalytic hydrogen-evolution experiments

The quartz reactor was irradiated with a 350 W mercury arc lamp (Oriel). The spectrum of the output light was adjusted by using a water filter and a cut-off filter (Newport). The photocatalysis was performed in a continuous-flow reactor system.<sup>[2]</sup> Within the inner compartment of a double-walled quartz tube (50 mL), polymeric carbon nitride (5 mg) was suspended in an aqueous solution of 10 vol% triethanolamine (TEOA) (20 mL) containing variable salts. Platinum metal (~3 %wt) was photo-deposited by addition of  $\text{H}_2\text{PtCl}_6$  at the beginning. The suspension was de-aerated by purging with argon for 1 hr before photo-irradiation. During the photocatalytic experiment, the suspension was continuously agitated by using a magnetic stirrer and kept cooled by running coolant water at 20 °C through the outer compartment. Argon was continuously purged through the suspension at a controlled flow rate (30 mL/min) to carry any hydrogen formed into a GC (Shimadzu GC-2014; sample loop 1 mL) equipped with a discharge ionization detector (Vici pulsed discharge detector D-4-I-SH14-R) for quantification of the hydrogen gas.

### Solid State NMR Spectroscopy

$^{13}\text{C}$  and  $^{15}\text{N}$  NMR MAS spectra of all carbon nitrides were acquired on a Bruker Avance III 300 MHz NMR spectrometer (7 T) at 75 and 30 MHz, respectively (UNSW). Samples were packed into 4 mm zirconia rotors for use in 4 mm H-X CPMAS probe on a 300 MHz system. All spectra were acquired at ambient probe temperature.

$^{13}\text{C}$  CPMAS spectra of carbon nitrides were typically acquired with the following parameters: MAS: 6.5 kHz, on the 300, relaxation delay 2-120 s; 2 ms contact pulse, ramped from 50 to 100% on the  $^1\text{H}$  channel;  $^1\text{H}$  90° pulse of 2.55  $\mu\text{s}$  (98 kHz) decoupling with SPINAL64; 256 scans were usually acquired for satisfactory signal to noise; total time from 12 min to 8.5 hr to acquire. 1-D  $^{15}\text{N}$  CPMAS spectra were acquired on the same samples and were typically acquired with the following parameters: MAS: 4 kHz, on a 300 system; relaxation delay 2-120 s; 2-8 ms contact pulse, ramped from 50 to 100% on the  $^1\text{H}$  channel;  $^1\text{H}$  90° pulse of 4 - 4.5  $\mu\text{s}$

(55 - 62.5 kHz) decoupling with SPINAL64; 2800-7000 scans were usually acquired for satisfactory signal to noise; total time from 3 - 8.5 hr to acquire. The TOSS (Total Suppression of Spinning Side Bands) pulse sequence was also employed with  $^{13}\text{C}$  and  $^{15}\text{N}$  data acquisition to distinguish the isotropic peaks from the side bands, and to suppress baseline artifacts.

$^{13}\text{C}$  SEDPMAS (Spin Echo Direct Polarisation) spectra of carbon nitrides were typically acquired with the following parameters: MAS: 12 kHz, on the 300, relaxation delay 5-1200 s;  $^{13}\text{C}$   $90^\circ$  excitation pulse of 4.5  $\mu\text{s}$ ; echo time 77  $\mu\text{s}$ ;  $^1\text{H}$   $90^\circ$  pulse of 4  $\mu\text{s}$  (98 kHz) for decoupling with SPINAL64; up to 1288 scans were usually acquired for satisfactory signal to noise; total time from 12 min to 85 hr to acquire.

All spectra were acquired at ambient probe temperature. Chemical shift referencing was achieved externally with  $^1\text{H}$  to solid DSS; with  $^{13}\text{C}$  to glycine carbonyl at 176 ppm; with  $^{15}\text{N}$  to  $[\text{NH}_4]_2\text{SO}_4$ , 24 ppm on the  $\text{NH}_3$  scale."

## DNP MAS NMR

DNP measurements were performed on a 400 MHz (9.4 T) Bruker AVANCE-III HD DNP system equipped with a 263 GHz gyrotron and a 3.2 mm 3-channel HXY MAS DNP probe tuned to  $^1\text{H}$ - $^{13}\text{C}$ - $^{15}\text{N}$ . MAS rates of 8 kHz, controlled by a Bruker MAS2 unit, were used for all samples. Sapphire 3.2 mm rotors with zirconia drive caps were used for cryogenic spinning; active sample volume was approximately 28  $\mu\text{L}$ . Typical LTMAS temperatures were 98 K for variable temperature (VT) gas, 105 K for bearing gas, and 104 K for drive gas.

Samples of CNK (ca. 30 mg) were finely ground repeatedly in an agate mortar and pestle to achieve uniform particle size. 30  $\mu\text{L}$  of 30 mM AMUPol solution in 30% glycerol- $\text{d}_8$ , 70%  $\text{D}_2\text{O}$  were added to wet the solid mass, followed by vigorous grinding to homogenize the mixture. The mortar was allowed to let stand at ambient temperature for approximately 10 minutes to give the solution time to soak into the particles. A standard powder funnel was used to transfer the impregnated solid into sapphire 3.2 mm DNP rotors. A fully packed rotor contained circa 40 mg of radical-solution-impregnated PCN.

Prior to NMR experiments on the carbon nitrides, gyrotron parameters were calibrated to yield a smooth power curve/enhancement profile, signal enhancement was checked at the experimental conditions using a U- $^{13}\text{C}$ ,  $^{15}\text{N}$  proline sample with 10 mM of AMUPol

in water/glycerol mixture (glycerol-d8/D<sub>2</sub>O/H<sub>2</sub>O, 60/30/10), yielding an enhancement factor of 230. All spectra were acquired with a recycle delay of 3 s. CP experiments were performed with a 10% tangential ramp, a <sup>1</sup>H 90° pulse of 2.5 μs (100 kHz), and with proton decoupling field strength of 100 kHz. The <sup>13</sup>C and <sup>15</sup>N NMR spectra are indirectly referenced to 4,4-dimethyl-4-silapentane-1-sulfonic acid and ammonium chloride, respectively.

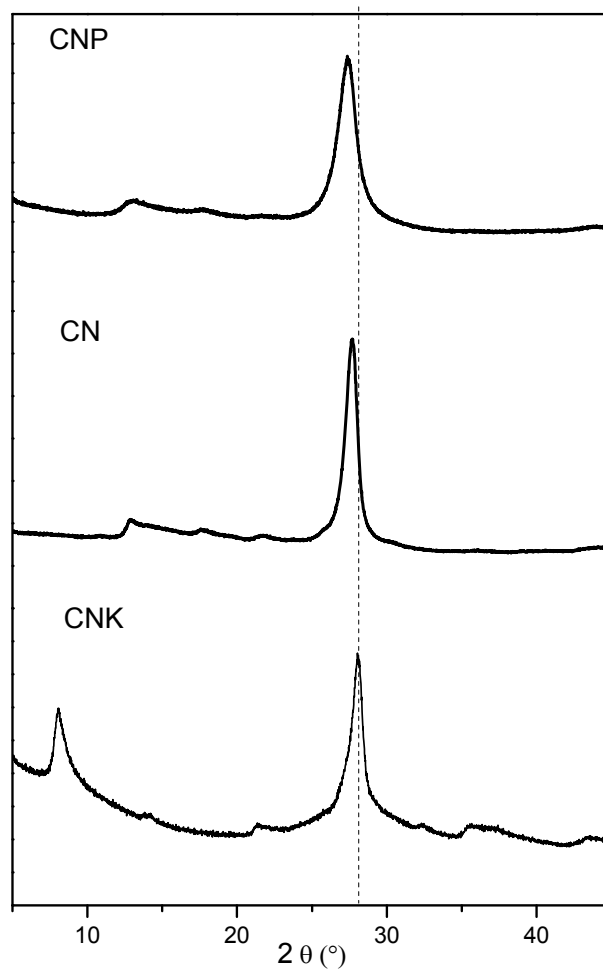


Figure S1. XRD patterns of conventional bulk polymeric carbon nitride (CN), porous polymeric carbon nitride (CNP) and CNK.

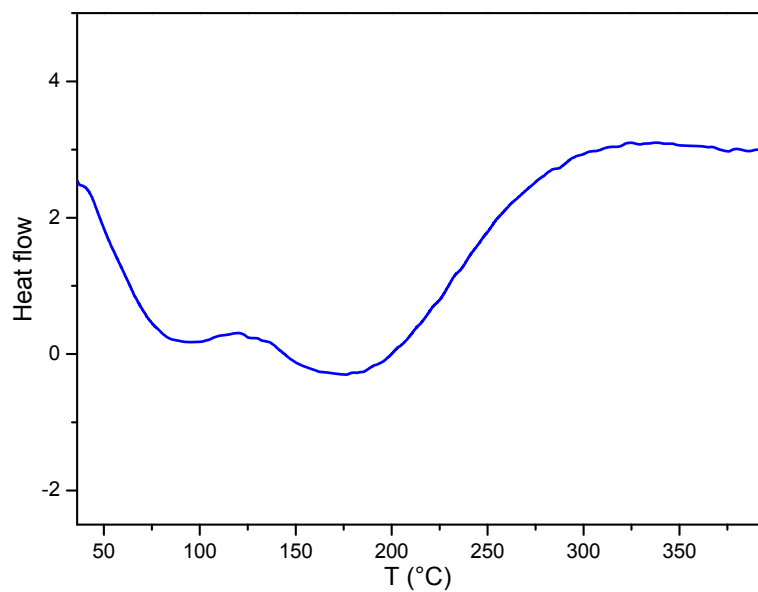
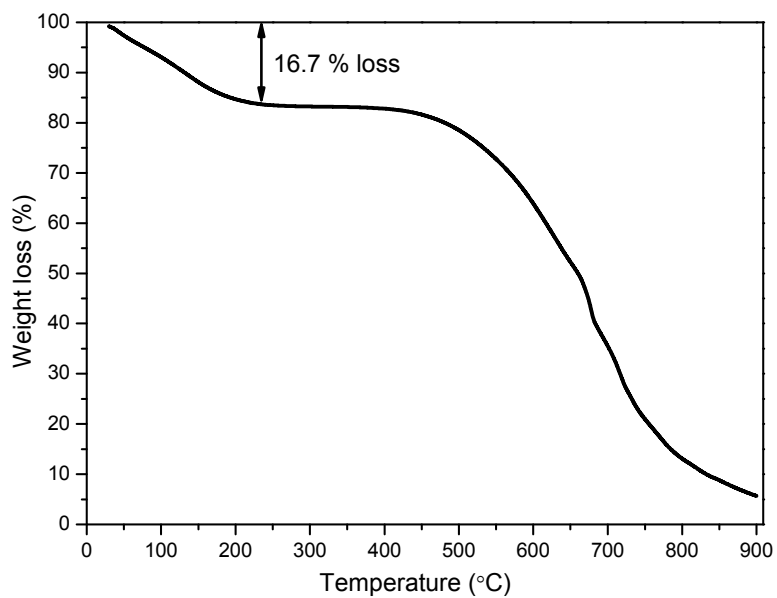


Figure S2. Thermogravimetric (top) and DSC (bottom) analysis of CNK in nitrogen.

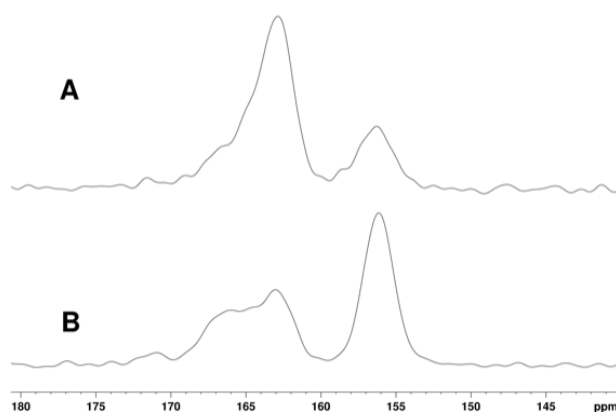


Figure S3. 75 MHz solid state  $^{13}\text{C}$  solid state MAS NMR spectra of CNK acquired with CP at 6.5 kHz MAS (A) and DP direct polarisation with high power decoupling at 12 kHz MAS (B).

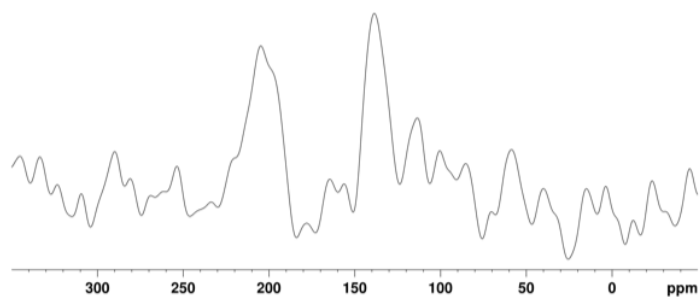


Figure S4. 30 MHz solid state  $^{15}\text{N}$  CPMAS NMR spectrum of CNK at 4kHz MAS.



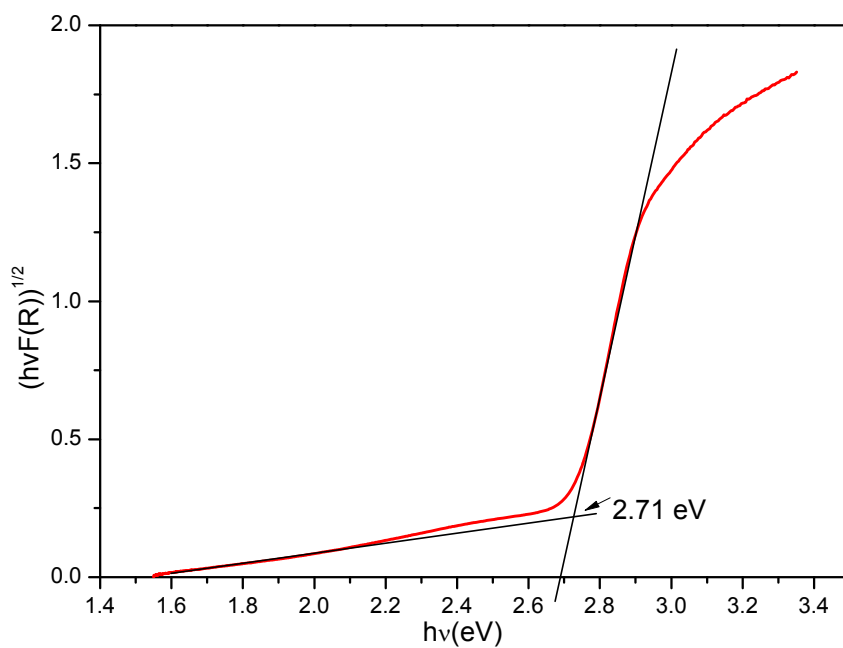
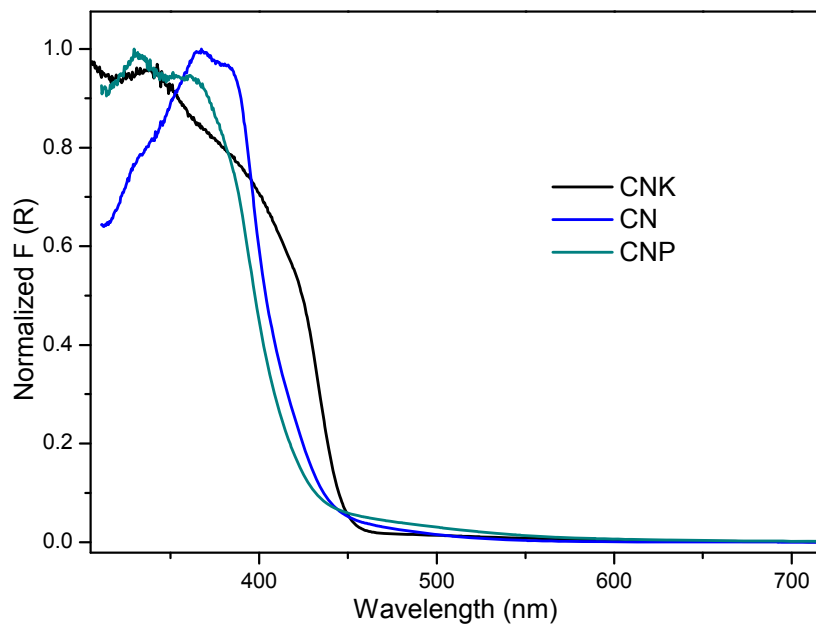


Figure S5. Solid state UV-vis diffuse reflectance spectra of CNK and conventional PCN materials (CN and CNP) (a), and Tauc-plot of CNK from the absorbance spectrum (b).

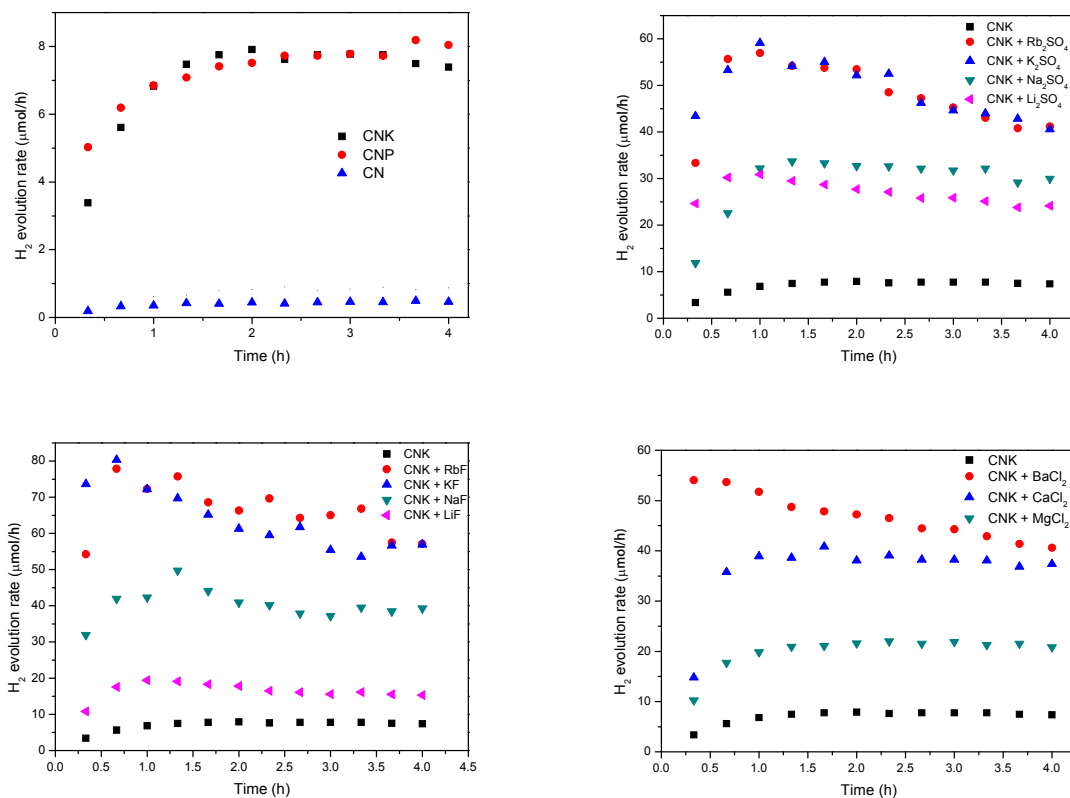


Figure S6. Photocatalytic hydrogen evolution rates of CNK, CNP and CN in the absence of salts in the reaction solution (a), and CNK in the presence of different salts in the reaction solution (b, c and d).

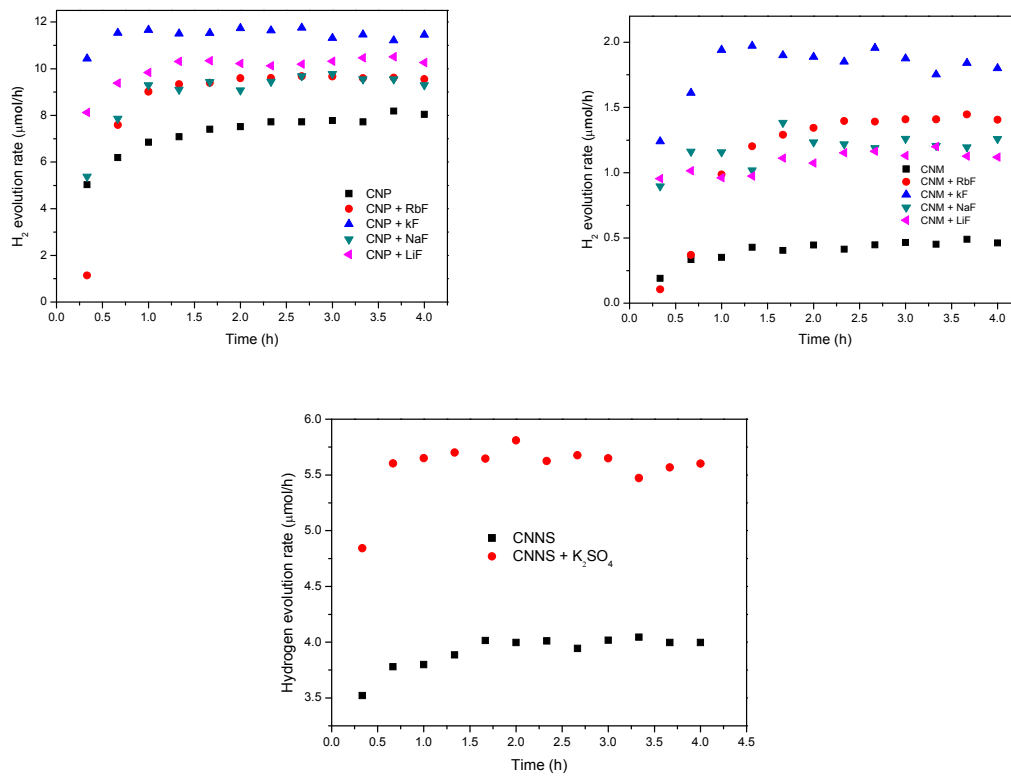


Figure S7. Photocatalytic hydrogen evolution rates of carbon nitrides in the presence of salts in the reaction solution, CNP (a), CNM (b), and CNNS (c).

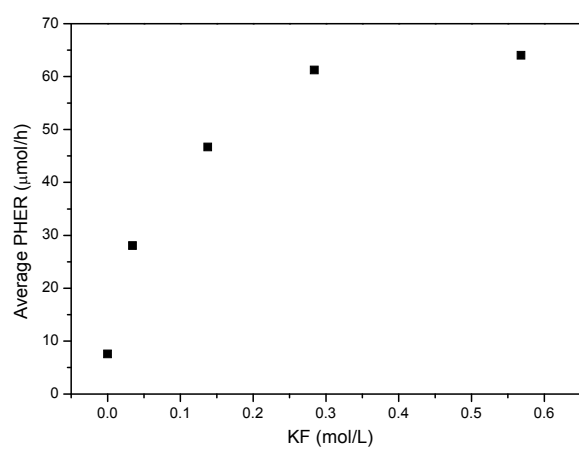
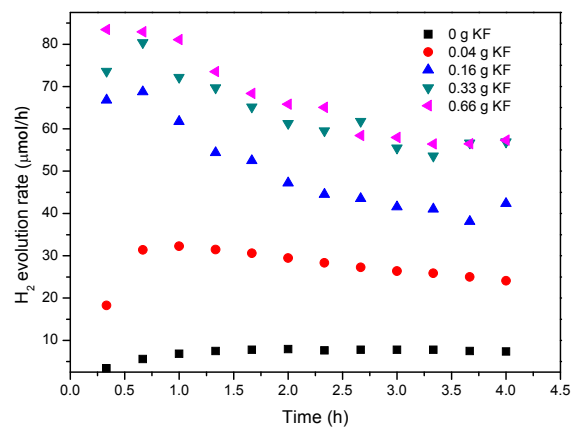


Figure S8. Photocatalytic hydrogen evolution of CNK in the presence of different amounts of potassium salt, KF

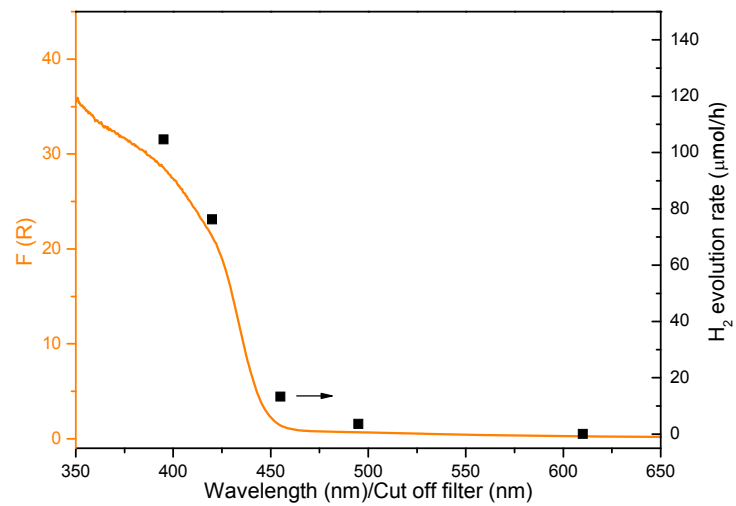


Figure S9. Action spectrum of CNK with different long-pass cut off filters.

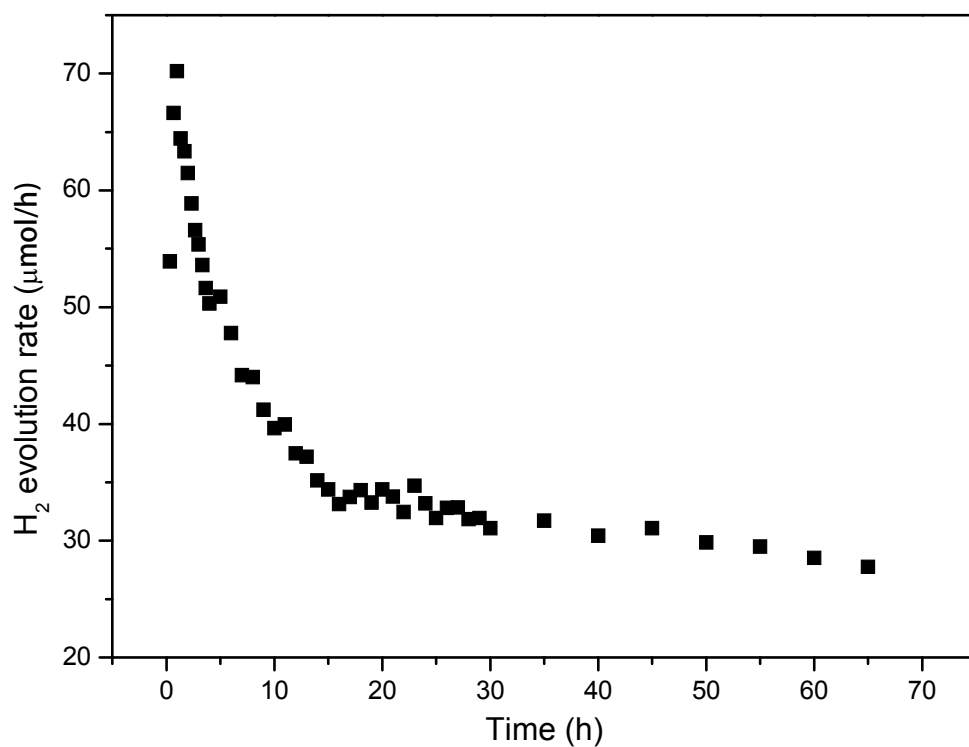


Figure S10. Long-term stability test of CNK in the presence of K<sup>+</sup> cations. Reaction conditions: 5 mg catalysts, 3 wt% photodeposited Pt, 20 mL H<sub>2</sub>O with 10 vol% triethanolamine (TEOA) and irradiation at  $\lambda > 420$  nm. The cation concentration is 0.287 M K (as the KF salt).

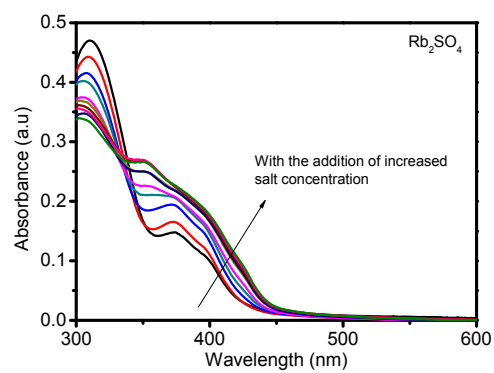
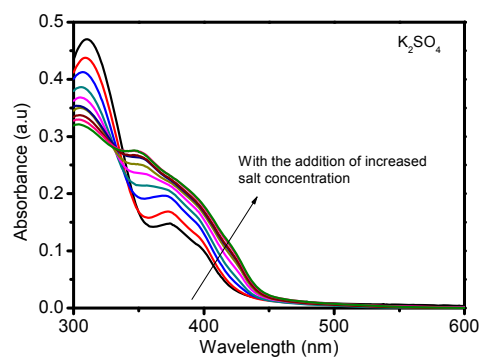
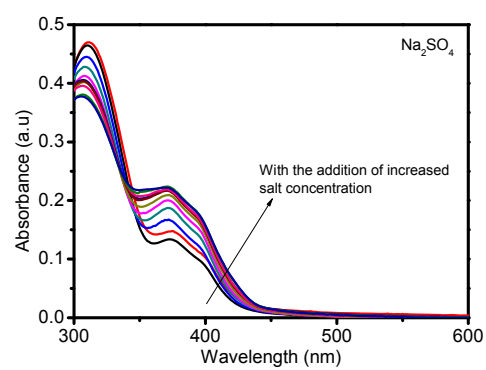
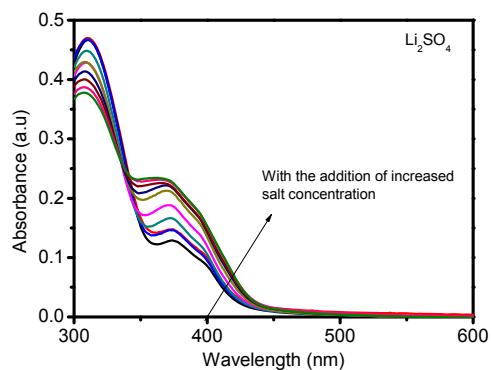


Figure S11. UV-vis spectra of CNK with increasing salt concentration from 48  $\mu\text{M}$  to 0.275 M.

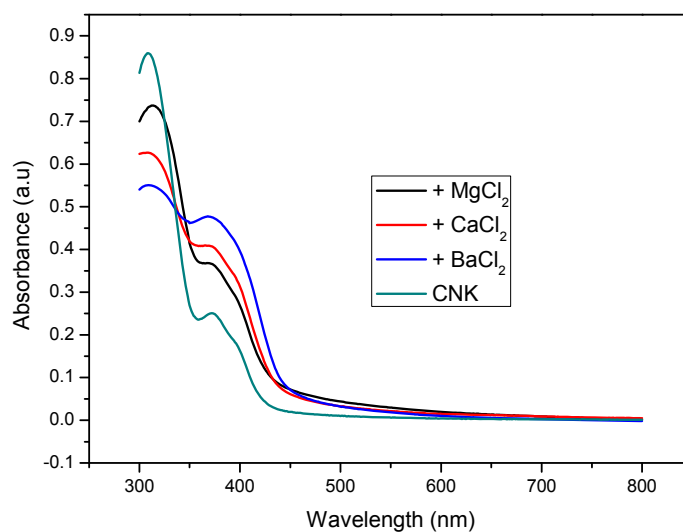


Figure S12. The UV-vis spectra of CNK in 10 wt% TEOA solution (photocatalytic reaction solution) in the presence of different chloride salts ( $\text{Mg}^{2+}$ ,  $\text{Ca}^{2+}$ , and  $\text{Ba}^{2+}$ ).

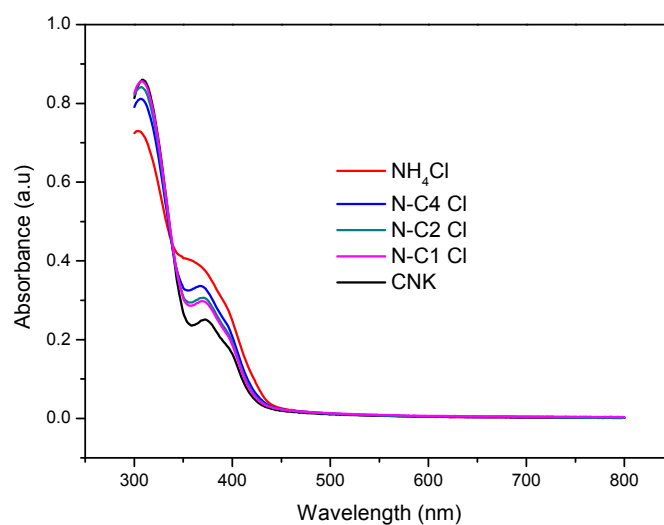


Figure S13. The UV-vis spectra of CNK in 10 wt% TEOA solution (photocatalytic reaction solution) in the presence of  $\text{NH}_4^+$  and quaternary ammonium cations ( N-C1: tetramethylammonium; N-C2: tetraethylammonium; N-C4: tetrabutylammonium).



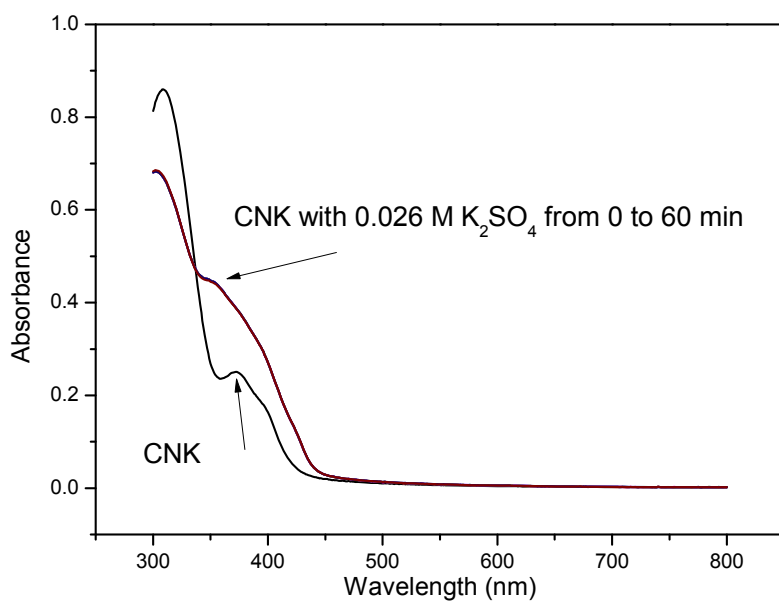


Figure S 14 .The 60 min UV-vis time course of CNK solution in the presence of 0.026 M  $K_2SO_4$ .

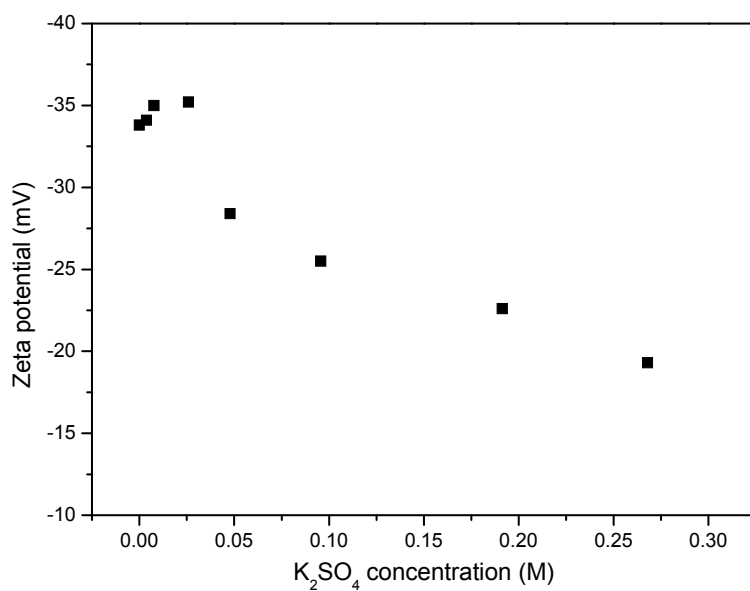


Figure S 15.  $K_2SO_4$  concentration dependent zeta potential of CNK.

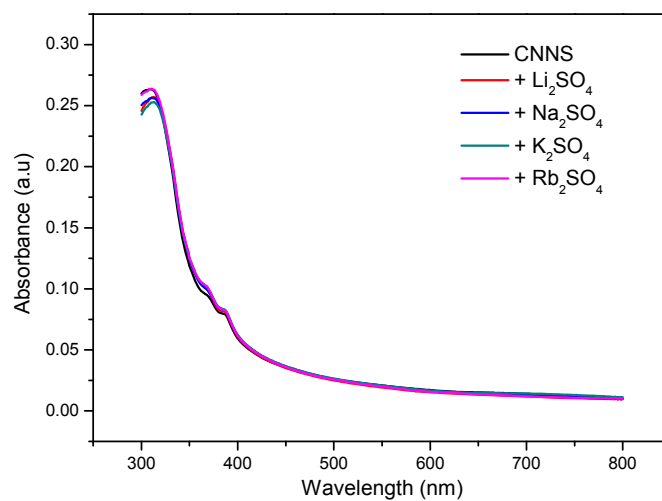


Figure S 16. The UV-vis spectra of CNNS in 10 wt% TEOA solution (photocatalytic reaction solution) in the presence of alkali chloride salts. The concentration of each cation is 0.275 M. Here, CNNS was chosen as it could be dispersed in 10 wt% TEOA solution for the solution UV-vis experiment.

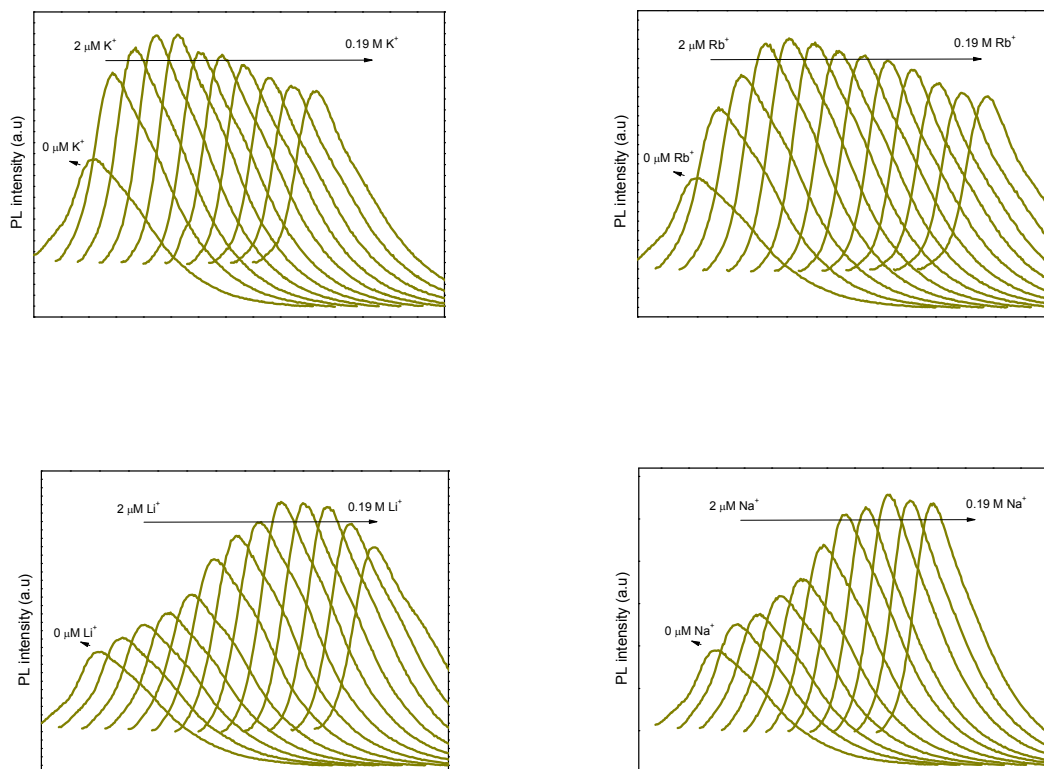


Figure S17. PL spectra of CNK in the photocatalytic reaction solution with the addition of varying concentrations of salts.

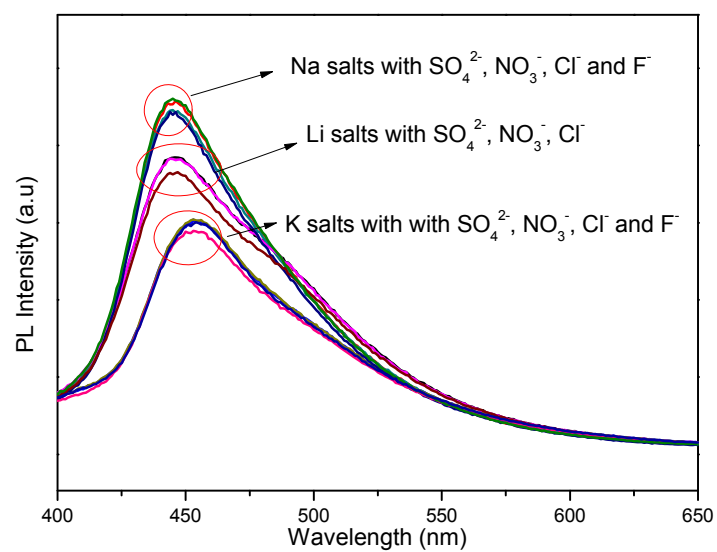


Figure S18. Anion effect on the PL spectroscopy.

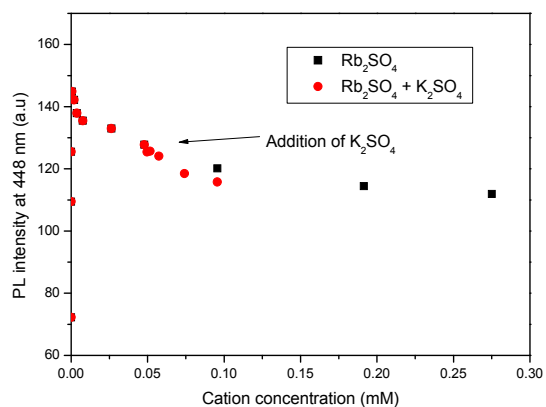
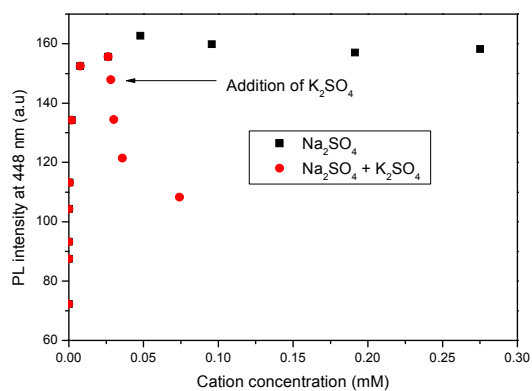
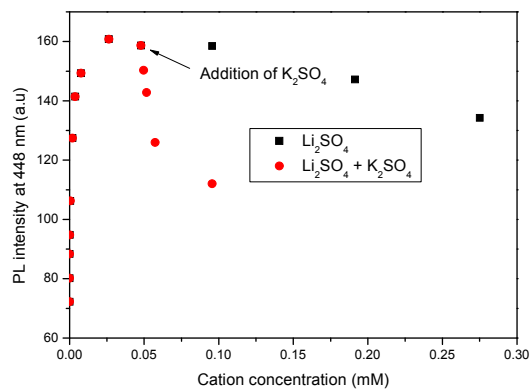


Figure S19 . The effect of potassium cations on the PL spectroscopy of CNK in the presence of  $\text{Rb}^+$  cations, and  $\text{Rb}^+$  and  $\text{K}^+$  cations

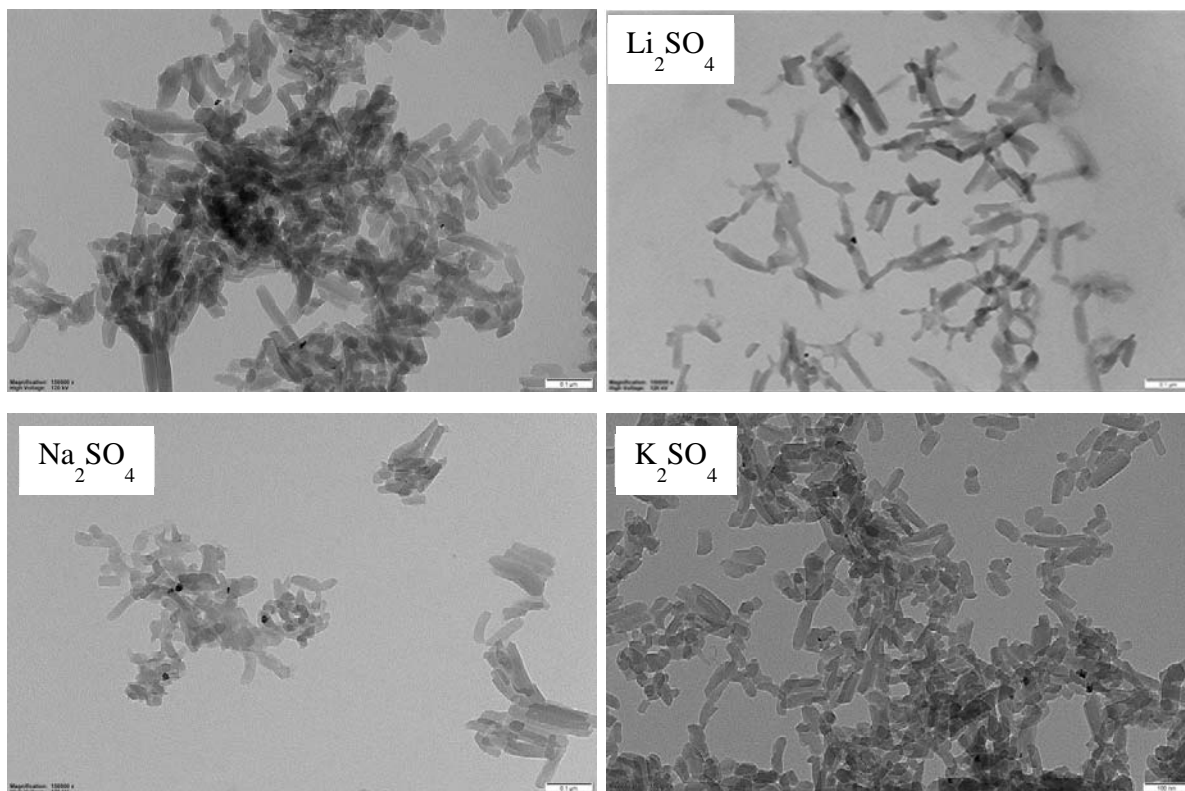


Figure S20. TEM images of CNK after photocatalytic hydrogen evolution with or without the addition of salts (scale bars 0.1  $\mu\text{m}$  and 100 nm for  $\text{K}_2\text{SO}_4$ ).

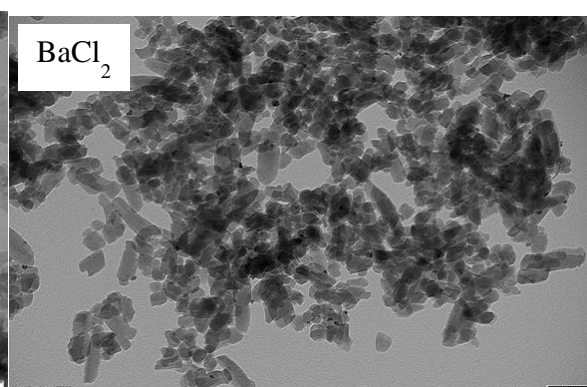
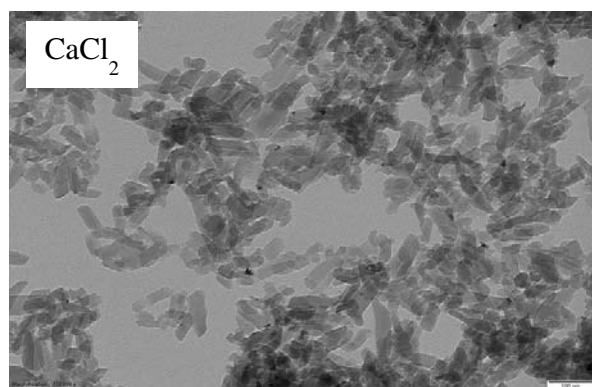
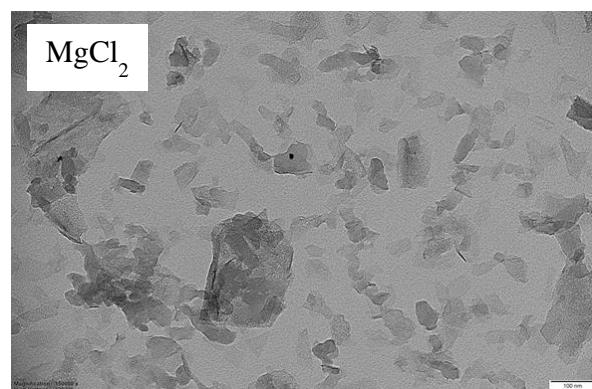


Figure S21. TEM images of CNK after photocatalytic hydrogen evolution with or without the addition of salts (scale bars 100 nm).

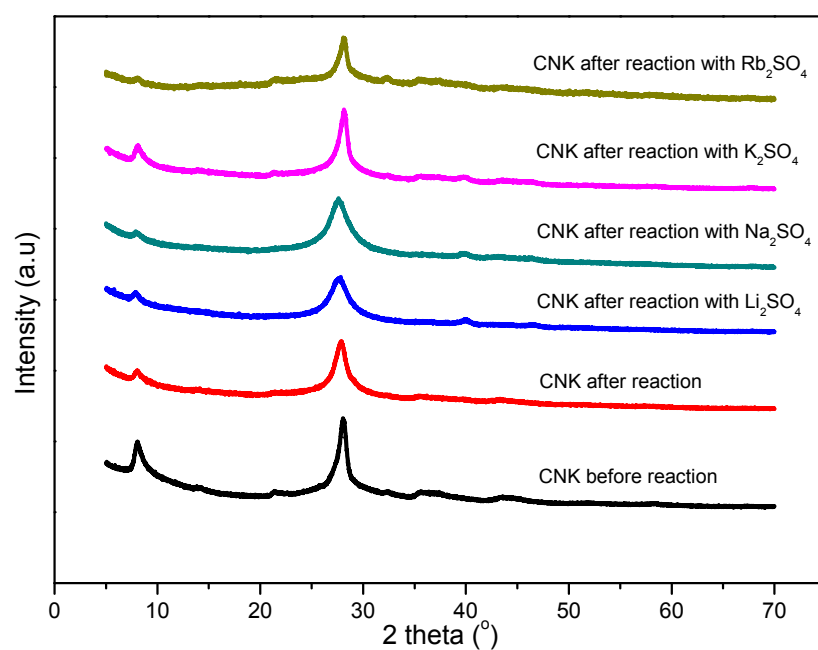


Figure S22. XRD patterns of CNK after photocatalytic hydrogen evolution with or without the addition of salts.



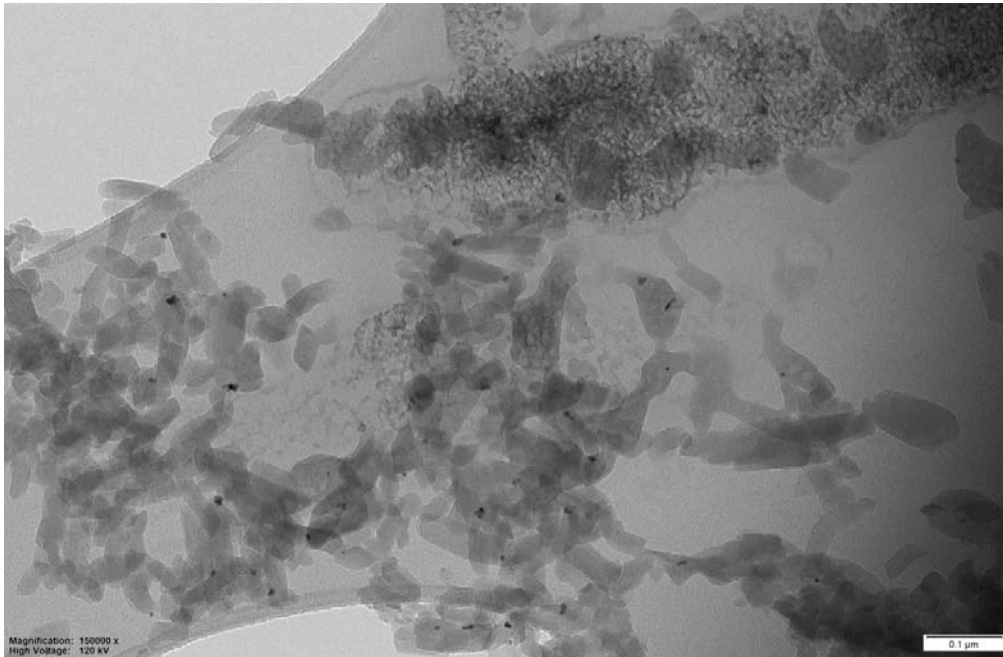


Figure S23. TEM image of CNK after long-term stability test in the presence of 0.287 M K (KF).

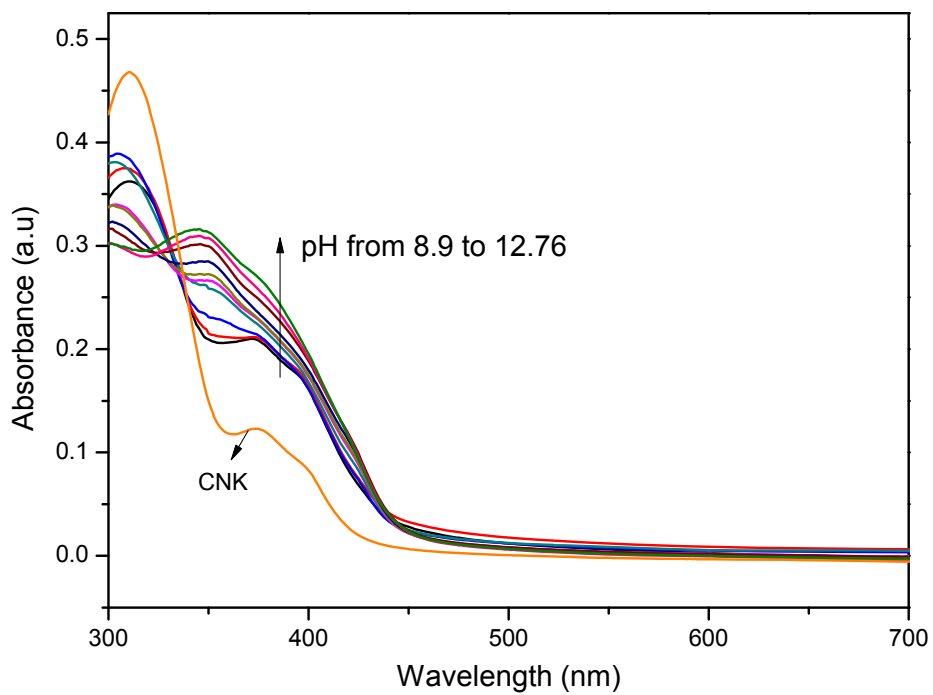


Figure S24. The effect of different pH on the UV-vis absorption of CNK in the photocatalytic hydrogen evolution reaction solution. The pH is adjusted with potassium phosphate salts, while fixing the potassium concentration at 0.275 M.

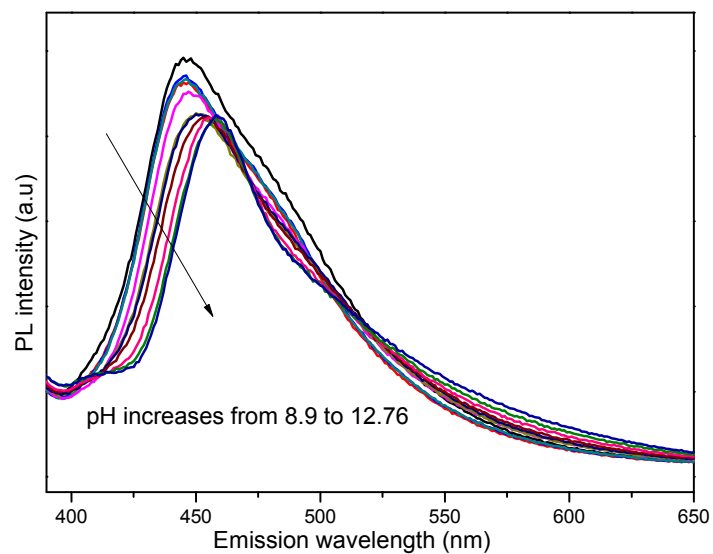


Figure S25. PL spectroscopy of CNK in the photocatalytic solution with adjusted pH.

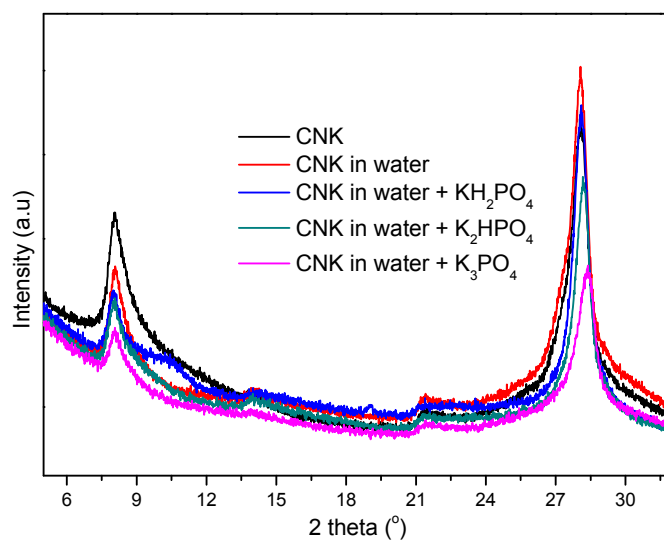


Figure S26. Slurry-state XRD of CNK in water with addition of potassium phosphate salts.

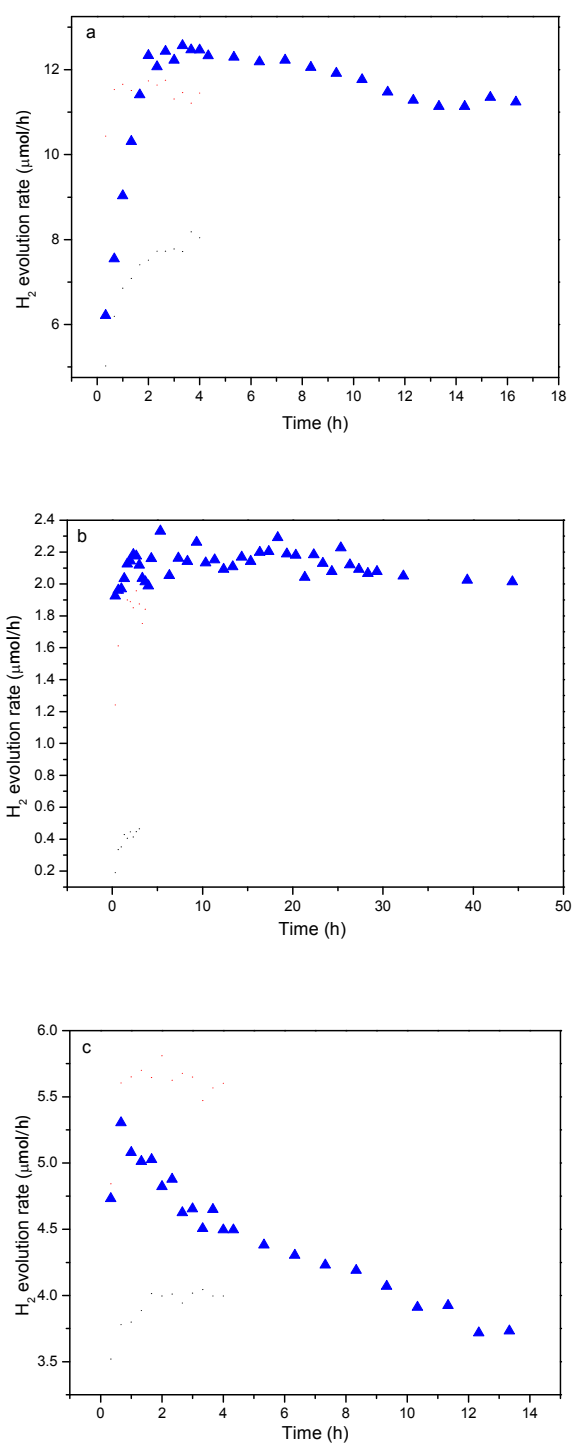


Figure S27. The effect of adding potassium phosphate salt to the reaction solution on the photocatalytic hydrogen evolution rate with conventional polymeric carbon nitrides, (a) CNP; (b) CN and (c) CNNS.

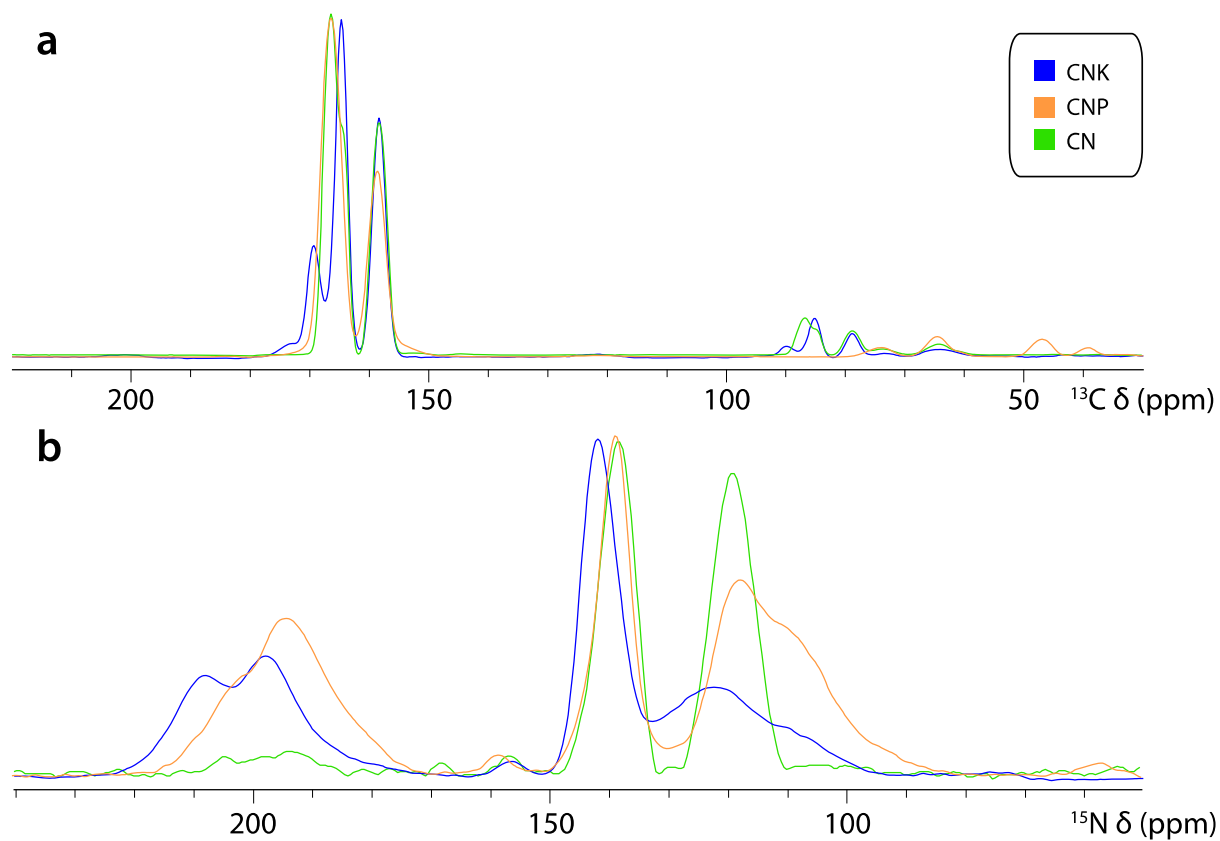


Figure S28. Comparison of DNP enhanced 1D  $^{13}\text{C}$  CP NMR spectra (a) and 1D  $^{15}\text{N}$  CP NMR (b) between CNK and other polymeric carbon nitrides, CNP and CN.

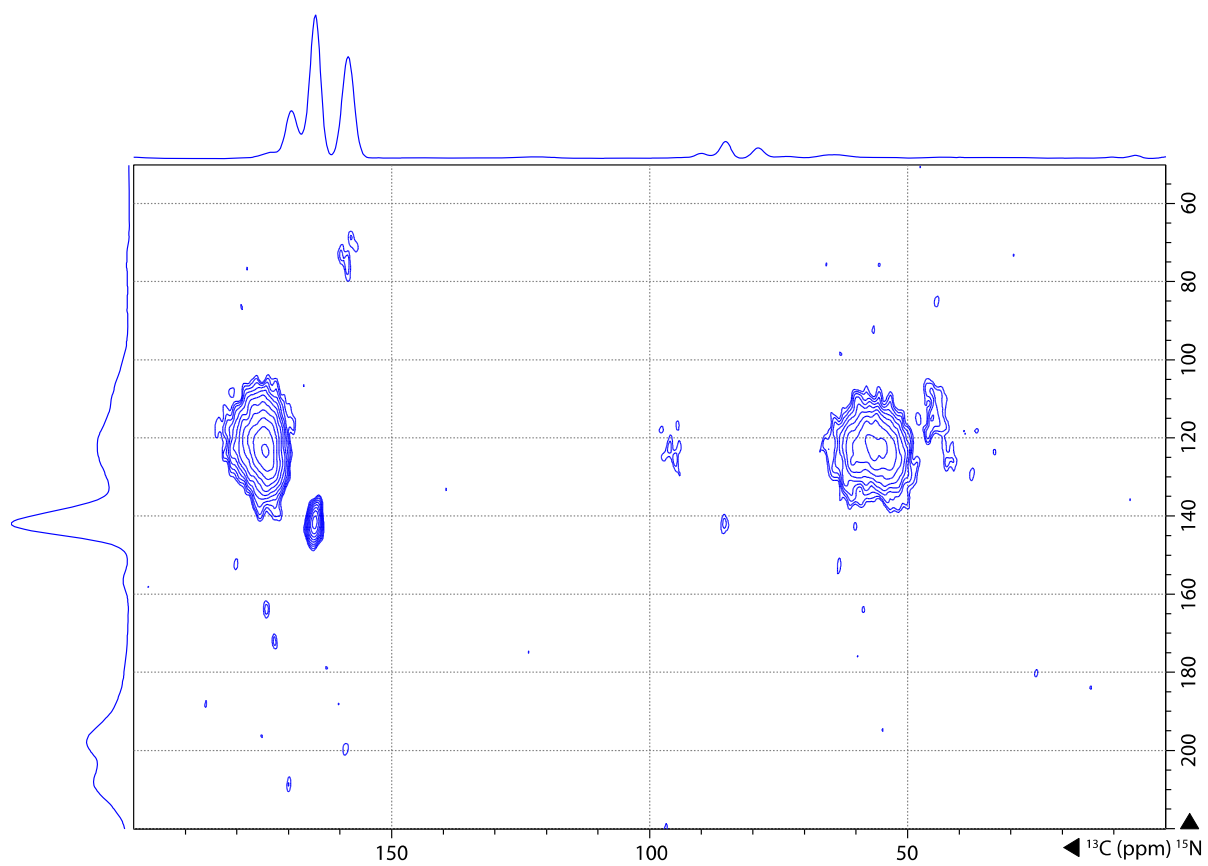


Figure S29. The DNP-enhanced 2D  $^{13}\text{C}$ - $^{15}\text{N}$  correlation spectrum (double-CP) of CNK at natural isotopic abundance.

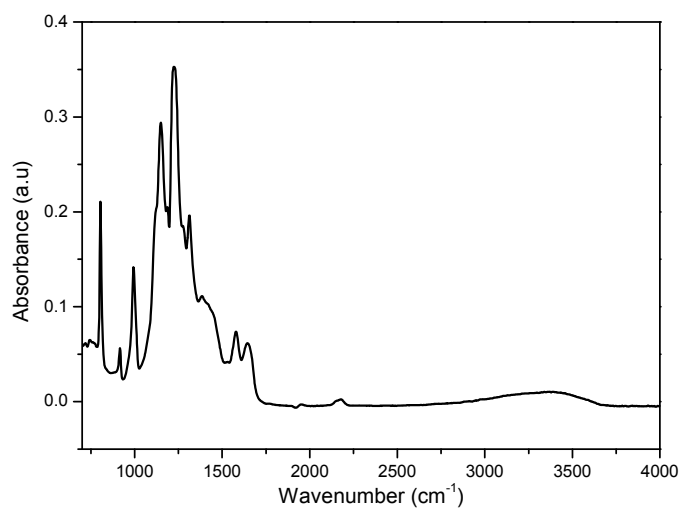


Figure S30. IR-ATR of CNK.

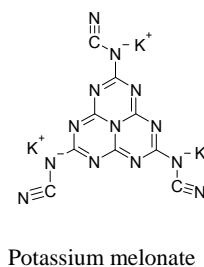
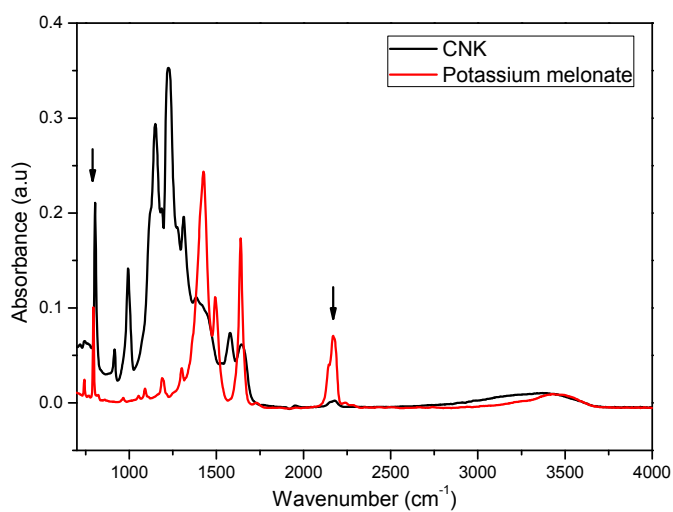


Figure S31. IR-ATR of CNK and potassium melonate. The height ratios of the  $2180\text{ cm}^{-1}$  signal (nitrile group) to the  $\sim 803\text{ cm}^{-1}$  absorption (from heptazine ring vibration) are 0.0375 and 0.73, respectively for CNK and potassium melonate. Each heptazine ring has 3 nitrile groups in potassium melonate, this gives 0.15 nitrile group for one heptazine on CNK.

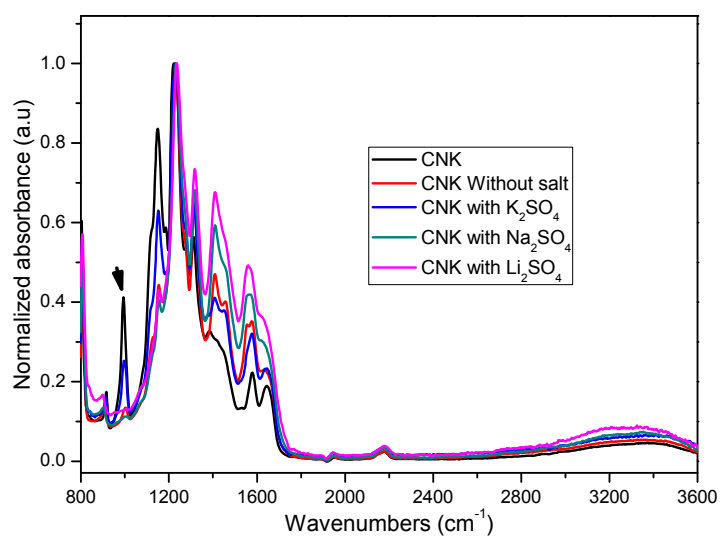


Figure S32. IR-ATR spectra of CNK after photocatalytic hydrogen evolution.



## Supporting information K EXAFS part

### X-ray Absorption Spectra

The Extended X-ray absorption fine structure (EXAFS) at the potassium K edge were measured at the Taiwan National Synchrotron Radiation Research Centre on beamline BL16A1. The X-ray data were collected with Si(111) monochromator crystal in Fluorescence mode at 10 K in vacuum. The raw data were analysed using the IFEFFIT 1.2.11 software package.

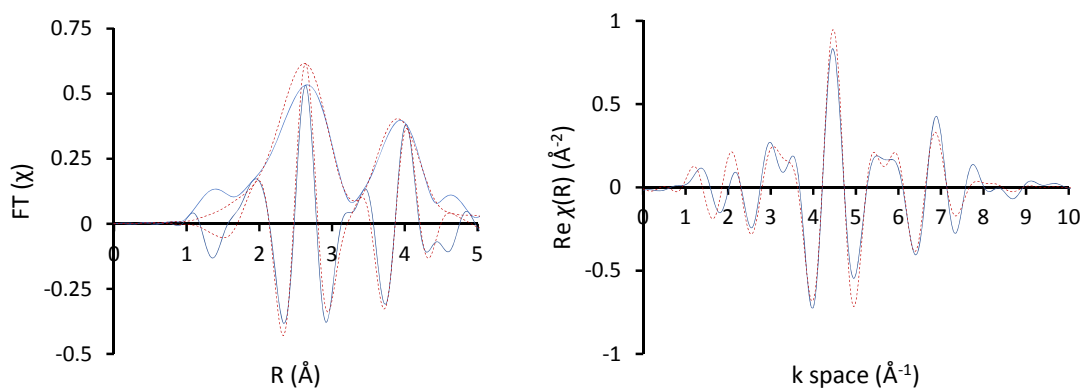


Figure S33. Potassium K Edge EXAFS data analysis with  $k^2$  weighting. Displaying KCl (Blue) and best fit (Red dash). Left – Fourier transform EXAFS; Right - inverse FT plot (R-range 1.3 – 5.0 Å).

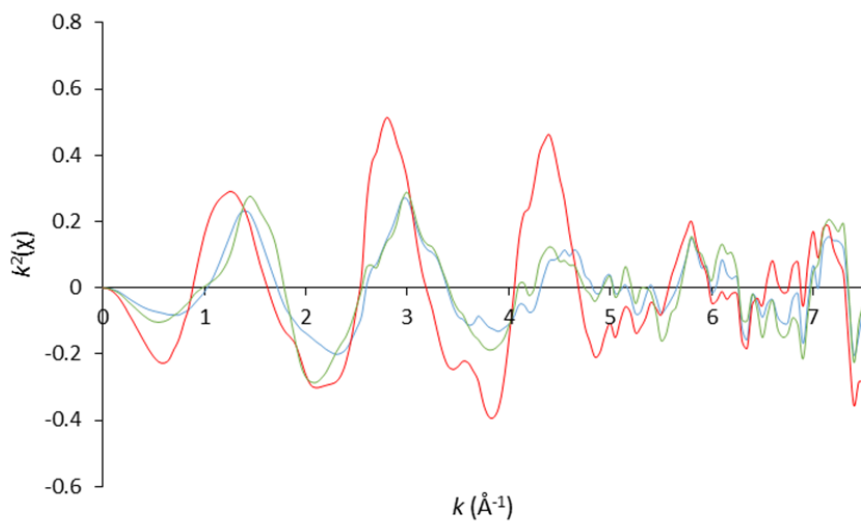


Figure S34. The normalised EXAFS spectra. Displaying CNK (Red); potassium melonate (blue) and potassium cyamelurate (green).

Table S1 Potassium K edge EXAFS fitting analysis of KCl data. (Error in brackets indicate variable)

Path (with Coordination)	Distance (Å)	Debye-Waller factor
6 K – Cl	3.10(3)	0.019(3)
12 K – K	4.42(2)	0.014(2)

$E_0 = 0(1)$ ; R-Factor = 0.010,  $S_{02} = 0.7$ ; k-range = 1.7 – 8.2; R-range = 1.3 – 5; k-weight = 3.

Table S2 Potassium K edge EXAFS fitting analysis of CNK data. (Error in brackets indicates variable)

Path (with Coordination)	Distance (Å)	Debye-Waller factor
1 K - N	2.56(4)	0.003(6)
5 K - N	2.83(2)	0.010(2)
2 K - K	4.34(3)	0.016(4)
2 K - K	5.09(3)	0.006(3)

$E_0 = -6(1)$ ; R-Factor = 0.006,  $S_{02} = 0.85$ ; k-range = 1.7 – 7.5; R-range = 1.6 – 5; k-weight = 2,3.

- [1] X. C. Wang, K. Maeda, X. F. Chen, K. Takanahe, K. Domen, Y. D. Hou, X. Z. Fu, M. Antonietti, *J. Am. Chem. Soc.* **2009**, *131*, 1680-1681.
- [2] E. Horvath-Bordon, E. Kroke, I. Svoboda, H. Fuess, R. Riedel, *New J. Chem.* **2005**, *29*, 693-699.
- [3] E. Kroke, M. Schwarz, E. Horath-Bordon, P. Kroll, B. Noll, A. D. Norman, *New J. Chem.* **2002**, *26*, 508-512.